Biogeosciences Discuss., 6, 6781–6802, 2009
www.biogeosciences-discuss.net/6/6781/2009/

Biogeosciences Discussions

Biogeosciences Discussions is the access reviewed discussion forum of *Biogeosciences*

Ocean acidification affects iron speciation in seawater

E. Breitbarth[1,2], R. J. Bellerby[1], C. C. Neill[1], M. V. Ardelan[4], M. Meyerhöfer[3], E. Zöllner[3], P. L. Croot[3], and U. Riebesell[3]

[1]Bjerknes Centre for Climate Research, University of Bergen, Bergen, Allégaten 55, 5007 Bergen, Norway
[2]Department of Chemistry, University of Otago, P.O. Box 56, Dunedin 9054, New Zealand
[3]Leibniz Institute of Marine Sciences (IFM-GEOMAR), Düsternbrooker Weg 20, 24105 Kiel, Germany
[4]Norwegian University of Science and Technology, Department of Chemistry, 7491 Trondheim, Norway

Received: 31 May 2009 – Accepted: 15 June 2009 – Published: 9 July 2009

Correspondence to: E. Breitbarth (ebreitbarth@chemistry.otago.ac.nz)

Published by Copernicus Publications on behalf of the European Geosciences Union.

Abstract

Rising atmospheric CO_2 is acidifying the surface ocean, a process which is expected to greatly influence the chemistry and biology of the future ocean. Following the development of iron-replete phytoplankton blooms in a coastal mesocosm experiment at 350, 700, and 1050 μatm pCO_2, we observed significant increases in dissolved iron concentrations, Fe(II) concentrations, and Fe(II) half-life times during and after the peak of blooms in response to CO_2 enrichment, suggesting increased iron bioavailability. If applicable to the open ocean this may provide a negative feedback mechanism to the rising atmospheric CO_2 by stimulating marine primary production.

1 Introduction

Paleoclimate data indicate significant effects from the deposition of iron in aeolian dust on ocean biogeochemistry with feedbacks on global climate (Watson et al., 2000). Studies of artificial and natural iron input have demonstrated iron control of phytoplankton productivity and CO_2 drawdown over vast oceanic regions (Boyd et al., 2007; Blain et al., 2007; Pollard et al., 2009) and in coastal upwelling regions (Bruland et al., 2001; Hutchins and Bruland, 1998). Temporal control of iron on phytoplankton productivity was also observed in a Norwegian fjord system (Öztürk et al., 2002). The Pelagic ecosystem CO_2 enrichment study (PeECE III) studied natural phytoplankton blooms under atmospheric CO_2 scenarios of 350, 700, and 1050 μatm pCO_2 in a coastal mesocosm experiment (Schulz et al., 2008). We used this unique opportunity to investigate the combined effects of phytoplankton bloom development and ocean acidification on Fe chemistry.

Iron solubility in surface seawater is low and the speciation is largely controlled by organic complexation and photochemical processes (Kuma et al., 1996; Sunda and Huntsman, 2003; Kuma et al., 1992). In addition to organic compounds generally present in coastal seawater, phytoplankton blooms can affect Fe(III)-complexation,

BGD

6, 6781–6802, 2009

which affects the dissolved Fe fraction and photoreactivity (Croot et al., 2001; Kuma et al., 1992; Rue and Bruland, 1995). Ligand production is generally facilitated via zooplankton and protist grazing, microbial production, and potentially also by phytoplankton cell degradation (Heldal et al., 1996; Barbeau et al., 1996; Hutchins and Bruland, 1994). In return, iron bioavailability differs among types of organic iron complexation and prokaryotic or eukaryotic phytoplankton (Hutchins et al., 1999). Fe(III)-complexation is interlinked with Fe(II) production in marine water, mainly via supplying the substrate for photoreduction in sunlit surface waters (Kuma et al., 1992; Öztürk et al., 2004; Barbeau et al., 2001; Barbeau et al., 2003). Fe(II) is generally considered bioavailable, but rapid reoxidation to Fe(III) in temperate waters result in limited concentrations. Half-life times range in the order of minutes and are largely dependent on temperature, oxygen and hydrogen peroxide concentrations, and pH (Santana-Casiano et al., 2005; Millero et al., 1987; Millero and Sotolongo, 1989), with presently limited knowledge about the role of organic Fe(II) complexation in natural seawater. However, the contribution of Fe(II) to phytoplankton nutrition may be significant in the open ocean (Roy et al., 2008) as well as in estuarine waters (Breitbarth et al., 2009).

Despite our growing knowledge of iron biogeochemistry in seawater, we currently have little information on the effects of ocean acidification thereon. Seawater pH affects phytoplankton physiology (Fu et al., 2008; Hare et al., 2008; Riebesell, 2004) and thus indirect effects via phytoplankton exudates that complex iron may also alter biological influences on iron solubility and cycling. Further, the photoreduction of organic Fe-ligand complexes is the main pathway for Fe(II) production in the euphotic zone (King et al., 1993) and moreover Fe(II) oxidation rates are strongly pH dependent (e.g. Santana-Casiano et al., 2005). For unabated CO_2 emissions, oceanic uptake of anthropogenic CO_2 will lower surface ocean pH from a pre-industrial 8.25 to an estimated 7.85 within this century, and further by up to 0.7 units until 2300 (Caldeira and Wickett, 2003; Jacobson, 2005). This change far exceeds any glacial-interglacial differences (Caldeira and Wickett, 2003) and thus may have profound effects on the biogeochemistry of iron in seawater. The PeECE III experiment offered a unique opportunity to study iron

BGD
6, 6781–6802, 2009

chemistry in phytoplankton blooms grown simultaneously at different pCO_2 concentrations. We particularly evaluate dissolved iron concentrations, as well as Fe(II) levels and oxidation rates over the course of the PeECE III mesocosm study and elucidate if ocean acidification may affect iron speciation in seawater.

2 Methods

The experimental work was carried out from 15 May through 09 June 2005 at the National Mesocosm Facility located at the Espeland Marine Biological Station at the Raunefjord (60.3° N, 5.2° E), University of Bergen, Norway. Nine polyethylene (PE) enclosures (2 m diameter, 10 m deep, hereafter called mesocosms), were moored to a raft about 200 m from shore. The mesocosms were capped with gastight and light transparent (95% UV permeability) tents. Atmospheric CO_2 concentrations within three mesocosms each were adjusted to 350, 700, and 1050 μatm pCO_2. Phytoplankton blooms were initiated with $NaNO_3$ and Na_2HPO_4 additions. The pH values are calculated based on daily measurements of total alkalinity (TA) and dissolved inorganic carbon (DIC) in the mesocosm upper mixed layer and are expressed on the total pH scale. TA was measured using the classical Gran electrotitration method (Gran, 1952) (precision $\pm 4 \mu$mol kg^{-1}). DIC was measured by coulometric titration (Johnson et al., 1987) with a precision of 2 μmol kg^{-1}. Chl-*a* concentrations were determined using HPLC (Barlow et al., 1997) and particulate organic carbon (POC) was measured on an elemental analyzer (EuroEA 3000, EuroVector) (Ehrhard and Koeve, 1999). Please see Schulz et al. (2008) for more details about the experimental set-up.

Total (tFe) and dissolved iron (dFe, 0.2 μm filtered) measurements were conducted using chemiluminescence flow injection analysis (CL-FIA, Waterville Analytical) (Bowie et al., 1998) and focused on the period of strong bloom development and pH shifts (days 7–13) and a past bloom measurement (day 23). Fe(II) was determined based on Croot and Laan (2002) using the same CL-FIA instrument, which was installed on the mesocosm raft for this purpose, during days 20 and 22 of the experiment. Samples

BGD
6, 6781–6802, 2009

were obtained from 2.5 m depth via syringe pumping through PTFE tubing, immediately followed by 0.2 μm filtration and injection into CL-FIA system. Additionally, Fe(II) oxidation rates were determined on 0.2 μm filtered samples form day 25 of the experiment, which were stored in the dark for 24 h to oxidize any Fe(II) present. Measurements were performed while having the samples, all reagents, and the sample loop of the flow injection analyzer immerged in a temperature controlled (10°C) water bath, in order to minimize analytical temperature effects during the measurements. The temperature was chosen as it is representative of the temperature inside the mesocosms during the study. The naperian log transformed chemiluminescent signal over time of 0.5, 0.75, and 1 nmol L^{-1} Fe(II) standard additions yield a linear signal decrease and the slope represents the Fe(II) oxidation rate constant (k_{ox} s^{-1}). Predicted Fe(II) oxidation rates were further calculated based on Millero et al. (1987) after calculating the [OH^-] concentration of the water using the CO_2SYS program (Lewis and Wallace, 1998), taking seawater carbonate chemistry measurements and oxygen concentrations into account.

3 Results and discussion

CO_2 perturbation and phytoplankton bloom development result in pH shifts from 7.67–7.97, 7.82–8.06, and 8.13–8.26 at 1050, 700, and 350 μatm pCO_2, respectively during days 3–12 and relatively constant levels thereafter (Figs. 1 and 2). The peak of the bloom is marked by Chl-*a* concentrations at days 9 (low CO_2) and 10 (mid and high CO_2) and results in particulate organic carbon (POC) concentrations peaking at days 10 (low CO_2, 91.9 μmol L^{-1}) and 11 (mid and high CO_2, 98.9 and 97.4 μmol L^{-1} respectively) (Figs. 1 and 2). Please see Schulz et al. (2008) for more details about the bloom development.

The Chl-*a* and POC biomasses in the three pCO_2 treatments are not markedly different. Nevertheless, our experiments show significantly higher dissolved iron (<0.2 μm, dFe) concentrations for high CO_2 treatments in comparison to the mid- and low CO_2 scenarios (e.g. 4.42 vs. 1.92 and 2.73 nmol L^{-1} on day 9, Fig. 3). During the bloom dFe

BGD
6, 6781–6802, 2009

decreases and reflects iron uptake in all treatments. Remineralization during bloom decline increases dFe levels again and dFe was maintained at significantly higher levels in the future scenario compared to the mid and low CO_2 treatments. Distinctions in dFe towards the end of the bloom (day 23, 2.8–4.2 nmol L^{-1} at low and mid CO_2, 6.0–8.2 nmol L^{-1} under high CO_2, Fig. 3) suggest differences in Fe remineralization in the treatments. Fe concentrations in the mesocosms were higher than in nearby fjord water (6.2 nmol L^{-1} total Fe (tFe) and 3.0 nmol L^{-1} dFe on day 13). Total Fe ranged from 23.7 to 96.1 nmol L^{-1} and varied between enclosures and over time. However, dissolved Fe values do not correlate with tFe and thus tFe concentrations are not responsible for the systematically increased dFe values in the high CO_2 treatments (Fig. 4). The total Fe data suggest an input of relatively unreactive particulate Fe during the filling process of the enclosures. Clearly, the mesocosms were Fe-replete and while we lack iron measurements from the start of the experiment, applying an Fe:C ratio of 65 μmol:mol (Sarthou et al., 2005) yields an iron demand of 2–6 nmol L^{-1} during the bloom, which approximates the iron detected in fjord water.

Any Fe(III)-hydroxide solubility change over the observed pH ranges during the iron measurements (7.77–8.21 up to 7.94–8.26, Fig. 2) is significantly lower than the observed differences in dFe suggesting biological iron-ligand production and colloid formation to be responsible for maintaining elevated dFe in the high CO_2 mesocosms (Kuma et al., 1996; Millero, 1998). Croot et al. (2001) show a ~2-fold Fe-ligand concentration increase resulting in rising dFe concentrations after 12–13 days iron induced phytoplankton bloom development. This was paralleled by a ~5-fold increase in chlorophyll-a biomass, similar to our study. Likewise, Croot et al. (2004) suggest a biological source of iron ligands in association with chlorophyll maxima in the water column. Further supporting the inclination that the increased dFe concentrations during the high CO_2 treatments are biologically controlled are associations of colloidal and organically complexed Fe fractions with phytoplankton blooms in Norwegian coastal waters (Öztürk et al., 2002, 2003), which may further be controlled by bacterial production of extracellular matrixes (Heldal et al., 1996).

BGD
6, 6781–6802, 2009

The pH decrease may affect iron-ligand complex stabilities, resulting in altered photolability of Fe(III)-ligand complexes (Lewis et al., 1995; Sunda and Huntsman, 2003). The future ocean scenarios showed higher Fe(II) values compared to the lower CO_2 treatments. Values between 52 and 411 pmol L^{-1} were detected, depending on treatment and time of day (Fig. 5). Due to fast moving cloud cover though, a clear diel cycle could not be determined. The solubility of Fe(II) is significantly greater than for Fe(III) and though while at these pH levels the oxidation of Fe(II) is still rapid (Santana-Casiano et al., 2006) it points towards an increase in the photolability of the iron organic complexes at lower pH (Sunda and Huntsman, 2003). Predictions of the Fe(II) half-life's over the course of the experiment reflect the expected pH dependence of Fe(II) oxidation rates (Fig. 6). The Fe(II) speciation shifts towards the Fe^{2+} ion below pH 8, while the oxidation rate is still largely controlled by $Fe(OH)_2$ (Santana-Casiano et al., 2006; Millero et al., 1995). Bloom dynamics cause pH shifts in the treatments that result in a much broader range of predicted Fe(II) half-life's in the high CO_2 treatments (3.4–20.6 min and 2.2–9.8 min, high and mid CO_2 respectively) vs. the low CO_2 treatment (1.1–2.6 min, Fig. 6). Especially during the early phase of the bloom, the relatively slow Fe(II) oxidation rates at low pH may aid in the bioavailability of iron via allowing for a larger standing stock of Fe(II). Dropping oxygen concentrations with bloom decline and organic matter remineralization after day 12 (by ~10% saturation overall) do not fully counteract acceleration effects on Fe(II) oxidation of the increasing temperature by ~0.5°C each on days 15 and 17 (Fig. 7). The product of both effects is visible in the parallel shift of the oxidation rate and resulting half-life times towards the lower end of the pH range of each treatment (Fig. 6). It should be noted that the contribution of hydrogen peroxide is not considered here, but may have implications when concentrations exceed 200 nmol L^{-1}, which is possible in coastal waters (Santana-Casiano et al., 2005). Temperature controlled Fe(II) oxidation rate measurements conducted at the end of the study reveal a decrease in oxidation rate from −0.81 to −1.02 min^{-1} (log K_{ox}) and result in an increase of Fe(II) half lives from 4.4–7.3 min in the pH range from 8.21–7.95 respectively. In comparison, estimates of the sole effect of pH on the Fe(II)

BGD
6, 6781–6802, 2009

half life in the same samples ranges from 1.5–5.1 min (Table 1). Similarly, predicted oxidation rates during the measurements in the mesocosms were faster than actual measured values (Fig. 5, Table 2). While the pH effect on inorganic Fe(II) speciation and thus on Fe(II) oxidation rates is clearly evident, the additional influence of phytoplankton bloom derivates on the actual half-life times are obvious. Hydrocarboxylic acids, such as glucaric acid, affect photoreduction of Fe(III) and may be released from phytoplankton (Kuma et al., 1992; Öztürk et al., 2004) while their direct effect on Fe(II) oxidation remains to be shown. The data suggest two possible mechanisms tying into Fe(II) cycling at different pH. Differences in oxidation rates and their deviation from the predicted rates indicate organic Fe(II)-complexation, which additionally may affect the Fe(II) half life in the low pH treatments stronger than in the high pH mesocosms. More so, biologically mediated Fe(III)-chelates supply the major pool of iron for photoreduction and this main Fe(II) production pathway (Boyd et al., 2000; Kuma et al., 1992) appears to operate more effectively at high CO_2 allowing for the elevated Fe(II) concentrations detected in the future ocean treatments. Effects thereof on biological production and remineralization may be profound.

Our study indicates that ocean acidification may lead to enhanced Fe-bioavailability due to an increased fraction of dFe and elevated Fe(II) concentrations in coastal systems due to pH induced changes in organic complexation and Fe(II) oxidation rates. Overall this will result in increased residence times for Fe in surface seawater leading ultimately to an enhancement of iron bioavailability since equilibrium partitioning eventually restores the biolabile Fe pools that have been depleted by biological uptake. These processes may further fuel increased phytoplankton carbon acquisition and export at future atmospheric CO_2 levels (Riebesell et al., 2007). Provided that the observed CO_2 sensitivity of iron chemistry represents a general phenomenon operating also in phytoplankton blooms of oceanic areas, it could have a profound effect on productivity in the future ocean (Blain et al., 2007; Boyd et al., 2007). Our results support the notion that changes in iron speciation and the resulting potential negative feedback mechanism of phytoplankton productivity on atmospheric CO_2 need to be

BGD
6, 6781–6802, 2009

considered when assessing the ecological effects of ocean acidification.

Acknowledgements. We gratefully acknowledge the help received from the staff of the Espeland Marine Biological Station, University of Bergen, Norway during the study. This work was partially funded through the MERCLIM project "Marine Ecosystem Response to a Changing Climate" (Norwegian Research Foundation (NFR), contract no. 184860/S30) and the University of Bergen LOCUS project. We further thank P. W. Boyd for his comments on the manuscript. E. B. especially thanks A. Aadnesen, as well as M. Hassellöv and D. R. Turner for their support and acknowledges current funding by the German Research Foundation (DFG, BR 3794).

References

Barbeau, K., Moffett, J. W., Caron, D. A., Croot, P. L., and Erdner, D. L.: Role of protozoan grazing in relieving iron limitation of phytoplankton, Nature, 380, 61–64, 1996.

Barbeau, K., Rue, E. L., Bruland, K. W., and Butler, A.: Photochemical cycling of iron in the surface ocean mediated by microbial iron(III)-binding ligands, Nature, 413, 409–413, 2001.

Barbeau, K., Rue, E. L., Trick, C. G., Bruland, K. T., and Butler, A.: Photochemical reactivity of siderophores produced by marine heterotrophic bacteria and cyanobacteria based on characteristic Fe(III) binding groups, Limnol. Oceanogr., 48, 1069–1078, 2003.

Barlow, R. G., Cummings, D. G., and Gibb, S. W.: Improved resolution of mono- and divinyl chlorophylls a and b and zeaxanthin and lutein in phytoplankton extracts using reverse phase C-8 HPLC, Mar. Ecol.-Prog. Ser., 161, 303–307, 1997.

Blain, S., Queguiner, B., Armand, L., Belviso, S., Bombled, B., Bopp, L., Bowie, A., Brunet, C., Brussaard, C., Carlotti, F., Christaki, U., Corbiere, A., Durand, I., Ebersbach, F., Fuda, J.-L., Garcia, N., Gerringa, L., Griffiths, B., Guigue, C., Guillerm, C., Jacquet, S., Jeandel, C., Laan, P., Lefevre, D., Lo Monaco, C., Malits, A., Mosseri, J., Obernosterer, I., Park, Y.-H., Picheral, M., Pondaven, P., Remenyi, T., Sandroni, V., Sarthou, G., Savoye, N., Scouarnec, L., Souhaut, M., Thuiller, D., Timmermans, K., Trull, T., Uitz, J., van Beek, P., Veldhuis, M., Vincent, D., Viollier, E., Vong, L., and Wagener, T.: Effect of natural iron fertilization on carbon sequestration in the Southern Ocean, Nature, 446, 1070–1074, 2007.

Bowie, A. R., Achterberg, E. P., Mantoura, R. F. C., and Worsfold, P. J.: Determination of sub-nanomolar levels of iron in seawater using flow injection with chemiluminescence detection, Anal. Chim. Acta, 361, 189–200, 1998.

Boyd, P. W., Watson, A. J., Law, C. S., and Abraham, E. R.: A mesoscale phytoplankton bloom in the polar Southern Ocean stimulated by iron fertilization, Nature, 407, 695–702, 2000.
Boyd, P. W., Jickells, T., Law, C. S., Blain, S., Boyle, E. A., Buesseler, K. O., Coale, K. H., Cullen, J. J., de Baar, H. J. W., Follows, M., Harvey, M., Lancelot, C., Levasseur, M., Owens, N. P. J., Pollard, R., Rivkin, R. B., Sarmiento, J., Schoemann, V., Smetacek, V., Takeda, S., Tsuda, A., Turner, S., and Watson, A. J.: Mesoscale Iron Enrichment Experiments 1993–2005: Synthesis and Future Directions, Science, 315, 612–617, doi:10.1126/science.1131669, 2007.
Breitbarth, E., Gelting, J., Walve, J., Hoffmann, L. J., Turner, D. R., Hassellöv, M., and Ingri, J.: Dissolved iron (II) in the Baltic Sea surface water and implications for cyanobacterial bloom development, Biogeosciences Discuss., 6, 3803–3850, 2009, http://www.biogeosciences-discuss.net/6/3803/2009/.
Bruland, K. W., Rue, E. L., and Smith, G. J.: Iron and macronutrients in California coastal upwelling regimes: Implications for diatom blooms, Limnol. Oceanogr., 46, 1661–1674, 2001.
Caldeira, K. and Wickett, M. E.: Anthropogenic carbon and ocean pH, Nature, 425, 365–365, 2003.
Croot, P. L., Bowie, A. R., Frew, R. D., Maldonado, M. T., Hall, J. A., Safi, K. A., La Roche, J., Boyd, P. W., and Law, C. S.: Retention of dissolved iron and Fe-II in an iron induced Southern Ocean phytoplankton bloom, Geophys. Res. Lett., 28, 3425–3428, 2001.
Croot, P. L. and Laan, P.: Continuous shipboard determination of Fe(II) in polar waters using flow injection analysis with chemiluminescence detection, Anal. Chim. Acta, 466, 261–273, 2002.
Croot, P. L., Andersson, K., Öztürk, M., and Turner, D. R.: The distribution and speciation of iron along 6° E in the Southern Ocean, Deep Sea Research Part II: Topical Studies in Oceanography, Oceanography, 51, 2857–2879, 2004.
Ehrhard, M. and Koeve, W.: Determination of particulate organic carbon and nitrogen, in: Methods of Seawater Analysis, edited by: Grasshoff, K., Kremling, K., and Ehrhard, M., Wiley-VCH, 437–444, 1999.
Fu, F.-X., Mulholland, M. R., Garcia, N. S., Beck, A., Bernhardt, P. W., Warner, M. E., Sañudo-Wilhelmy, S. A., and Hutchins, D. A.: Interactions between changing pCO_2, N_2 fixation, and Fe limitation in the marine unicellular cyanobacterium *Crocosphaera*, Limnol. Oceanogr., 53, 2472–2484, 2008.
Gran, G.: Determination of the equivalence point in potentiometric titrations of seawater with hydrochloric acid, Oceanol. Acta, 5, 209–218, 1952.

Hare, C. E., Leblanc, K., DiTullio, G. R., Kudela, R. M., Hutchins, D. A., Zhang, Y., Lee, P. A., and Riseman, S.: Consequences of increased temperature and CO_2 for phytoplankton community structure in the Bering Sea, Mar. Ecol.-Prog. Ser., 352, 9–16, 2008.
Heldal, M., Fagerbakke, K. M., Tuomi, P., and Bratbak, G.: Abundant populations of iron and manganese sequestering bacteria in coastal water, Aquat. Microb. Ecol., 11, 127–133, 1996.
Hutchins, D. A. and Bruland, K. W.: Grazer-mediated regeneration and assimilation of Fe, Zn and Mn from planktonic prey, Mar. Ecol.-Prog. Ser., 110, 259–269, 1994.
Hutchins, D. A. and Bruland, K. W.: Iron-limited diatom growth and Si : N uptake ratios in a coastal upwelling regime, Nature, 393, 561–564, 1998.
Hutchins, D. A., Witter, A. E., Butler, A., and Luther III, G. W.: Competition among marine phytoplankton for different chelated iron species, Nature, 400, 858–861, 1999.
Jacobson, M. Z.: Studying ocean acidification with conservative, stable numerical schemes for nonequilibrium air-ocean exchange and ocean equilibrium chemistry, J. Geophys. Res.-Atmos., 110, D07302, doi:07310.01029/02004JD005220, 2005.
Johnson, K. M., Williams, P. J., Brandstrom, L., and Sieburth, J. M.: Coulometric total carbon analysis for marine studies: automation and calibration, Mar. Chem., 21, 117–133, 1987.
King, D. W., Aldrich, R. A., and Charnecki, S. E.: Photochemical Redox Cycling of Iron in Nacl Solutions, Mar. Chem., 44, 105–120, 1993.
Kuma, K., Nakabayashi, S., Suzuki, Y., Kudo, I., and Matsunaga, K.: Photo-Reduction of Fe (III) by Dissolved Organic-Substances and Existence of Fe (II) in Seawater During Spring Blooms, Mar. Chem., 37, 15–27, 1992.
Kuma, K., Nishioka, J., and Matsunaga, K.: Controls on iron(III) hydroxide solubility in seawater: The influence of pH and natural organic chelators, Limnol. Oceanogr., 41, 396–407, 1996.
Lewis, B. L., Holt, P. D., Taylor, S. W., Wilhelm, S. W., Trick, C. G., Butler, A., and Luther III, G. W.: Voltammetric estimation of iron(III) thermodynamic stability constants for catecholate siderophores isolated from marine bacteria and cyanobacteria, Mar. Chem., 50, 179–188 1995.
Lewis, E. and Wallace, D. W. R.: Program Developed for CO_2 System Calculations. ORNL/CDIAC-105. Carbon Dioxide Information Analysis Center, Oak Ridge National Laboratory, US Department of Energy, Oak Ridge, Tenessee, 1998.
Millero, F. J., Sotolongo, S., and Izaguirre, M.: The oxidation kinetics of Fe(II) in seawater, Geochim. Cosmochim. Ac., 51, 793–801, 1987.
Millero, F. J. and Sotolongo, S.: The oxidation of Fe(II) with H_2O_2in seawater, Geochim. Cos-

mochim. Ac., 53, 1867–1873, 1989.
Millero, F. J., Yao, W. S., and Aicher, J.: The Speciation of Fe(II) and Fe(III) in Natural-Waters, Mar. Chem., 50, 21–39, 1995.
Millero, F. J.: Solubility of Fe(III) in seawater, Earth Planet. Sc. Lett., 154, 323–329, 1998.
Öztürk, M., Steinnes, E., and Sakshaug, E.: Iron Speciation in the Trondheim Fjord from the Perspective of Iron Limitation for Phytoplankton, Estuarine, Coast. Shelf Sc., 55, 197–212, 2002.
Öztürk, M., Vadstein, O., and Sakshaug, E.: The effects of enhanced phytoplankton production on iron speciation and removal in mesocosm experiments in a landlocked basin of Hopavagen, Norway, Mar. Chem., 84, 3–17, 2003.
Öztürk, M., Croot, P. L., Bertilsson, S., Abrahamsson, K., Karlson, B., David, R., Fransson, A., and Sakshaug, E.: Iron enrichment and photoreduction of iron under UV and PAR in the presence of hydroxycarboxylic acid: implications for phytoplankton growth in the Southern Ocean, Deep Sea Research Part II: Topical Studies in Oceanography, Oceanography, 51, 2841–2856, 2004.
Pollard, R. T., Salter, I., Sanders, R. J., Lucas, M. I., Moore, C. M., Mills, R. A., Statham, P. J., Allen, J. T., Baker, A. R., Bakker, D. C. E., Charette, M. A., Fielding, S., Fones, G. R., French, M., Hickman, A. E., Holland, R. J., Hughes, J. A., Jickells, T. D., Lampitt, R. S., Morris, P. J., Nedelec, F. H., Nielsdottir, M., Planquette, H., Popova, E. E., Poulton, A. J., Read, J. F., Seeyave, S., Smith, T., Stinchcombe, M., Taylor, S., Thomalla, S., Venables, H. J., Williamson, R., and Zubkov, M. V.: Southern Ocean deep-water carbon export enhanced by natural iron fertilization, Nature, 457, 577–580, 2009.
Riebesell, U.: Effects of CO_2 enrichment on marine phytoplankton, J. Oceanogr., 60, 719–729, 2004.
Riebesell, U., Schulz, K. G., Bellerby, R. G. J., Botros, M., Fritsche, P., Meyerhofer, M., Neill, C., Nondal, G., Oschlies, A., Wohlers, J., and Zollner, E.: Enhanced biological carbon consumption in a high CO_2 ocean, Nature, 450, 545–548, doi:10.1038/nature06267, 2007.
Roy, E. G., Wells, M. L., and King, D. W.: Persistence of iron(II) in surface waters of the western subarctic Pacific, Limnol. Oceanogr., 53, 89–98, 2008.
Rue, E. L. and Bruland, K. W.: Complexation of iron(III) by natural organic ligands in the Central North Pacific as determined by a new competitive ligand equilibration/adsorptive cathodic stripping voltammetric method, Mar. Chem., 50, 117–138, 1995.
Santana-Casiano, J. M., Gonzalez-Davila, M., and Millero, F. J.: Oxidation of Nanomolar Levels

of Fe(II) with Oxygen in Natural Waters, Environ. Sci. Technol., 39, 2073–2079, 2005.
Santana-Casiano, J. M., Gonzalez-Davila, M., and Millero, F. J.: The role of Fe(II) species on the oxidation of Fe(II) in natural waters in the presence of O_2 and H_2O_2, Mar. Chem., 99, 70–82, 2006.
Sarthou, G., Timmermans, K. R., Blain, S., and Treguer, P.: Growth physiology and fate of diatoms in the ocean: a review, J. Sea Res., 53, 25–42, 2005.
Schulz, K. G., Riebesell, U., Bellerby, R. G. J., Biswas, H., Meyerhöfer, M., Müller, M. N., Egge, J. K., Nejstgaard, J. C., Neill, C., Wohlers, J., and Zöllner, E.: Build-up and decline of organic matter during PeECE III, Biogeosciences, 5, 707–718, 2008, http://www.biogeosciences.net/5/707/2008/.
Sunda, W. and Huntsman, S.: Effect of pH, light, and temperature on Fe-EDTA chelation and Fe hydrolysis in seawater, Mar. Chem., 84, 35–47, 2003.
Watson, A. J., Bakker, D. C. E., Ridgwell, A. J., Boyd, P. W., and Law, C. S.: Effect of iron supply on Southern Ocean CO_2 uptake and implications for glacial atmospheric CO_2, Nature, 407, 730–733, 2000.

Table 1. FE oxidation rates and half lifes at 10°C for oxygen saturated seawater after incubation the mesocosms for 25 days compared with FE oxidation rates estimated based on Millero et al. (1987).

	measured			predicted	
pH_{total}	log k_{ox} (min^{-1})	s. d.	t $\frac{1}{2}$ (min)	log k_{ox} (min^{-1})	t $\frac{1}{2}$ (min)
8.214	−0.81	0.12	4.4	−0.35	1.5
8.015	−0.90	0.07	5.4	−0.73	3.8
7.950	−1.02	0.05	7.3	−0.86	5.1

BGD
6, 6781–6802, 2009

Table 2. Fe(II) oxidation rates and half lifes in the mesocosms during mid-day in synchronization with carbonate system measurements on day 11 and day 13 compared with Fe(II) oxidation rates estimated based on Millero et al. (1987). See also Fig. 5 for the respective Fe(II) concentrations measured.

			measured			predicted	
day	pH total	T (°C)	O_2 (μmol L^{-1})	log k_{ox} (min^{-1})	$t_{\frac{1}{2}}$ (min)	log k_{ox} (min^{-1})	$t_{\frac{1}{2}}$ (min)
20	8.20	11.5	287.6	−0.90	5.5	−0.26	1.3
20	8.00	11.6	297.1	−1.21	11.2	−0.64	3.0
20	7.97	11.6	311.3	−1.24	12.0	−0.69	3.4
22	8.23	10.5	291.2	−0.96	6.3	−0.31	1.4
22	8.03	10.7	297.2	−1.18	10.4	−0.67	3.3
22	7.98	10.6	305.4	−1.21	11.2	−0.78	4.2

BGD
6, 6781–6802, 2009

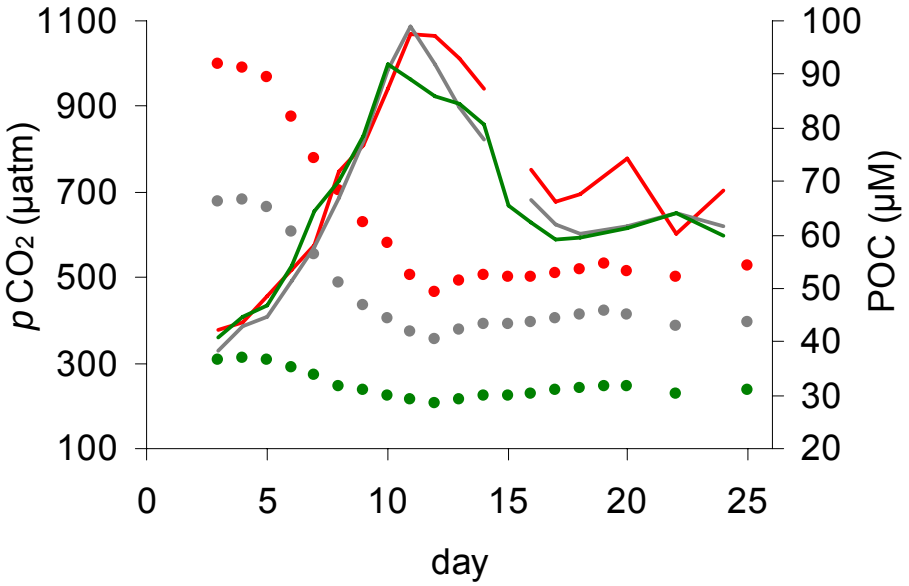

Fig. 1. Development of pCO_2 (symbols) and POC (lines) over the course of the mesocosm experiment shown as the mean values of the high (red), mid (grey), and low CO_2 (green) treatments. See Schulz et al. (2008) for the complete data set.

BGD
6, 6781–6802, 2009

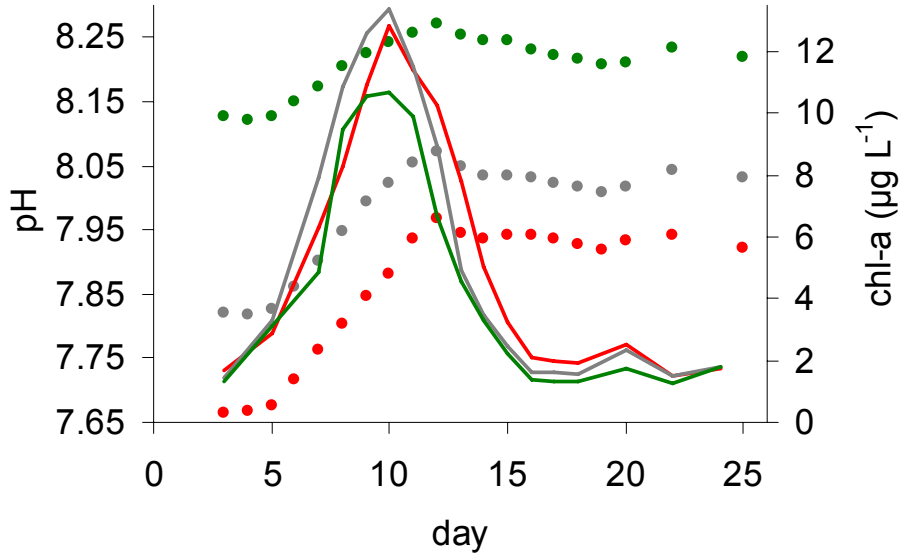

Fig. 2. Development of pH (symbols) and Chl-a (lines) over the course of the mesocosm experiment shown as the mean values of the high (red), mid (grey), and low CO_2 (green) treatments. See Schulz et al. (2008) for the complete data set.

BGD
6, 6781–6802, 2009

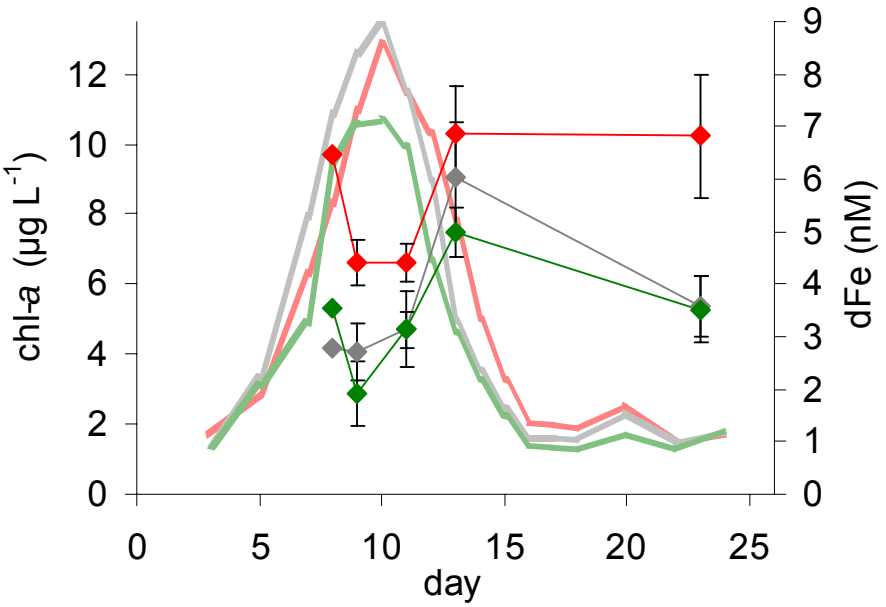

Fig. 3. Mean dFe concentrations (symbols, error bars denote standard deviations) and mean Chl-*a* concentrations (lines) during the mesocosm experiment at high (red), mid (grey), and low CO_2 (green).

BGD
6, 6781–6802, 2009

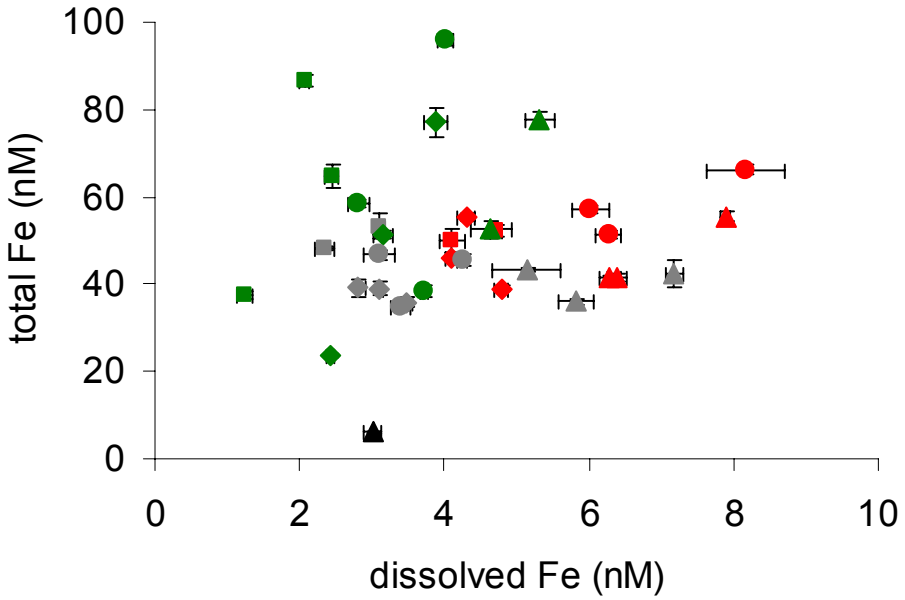

Fig. 4. dFe concentrations plotted versus tFe concentrations during the mesocosm experiment. High CO_2=red, mid CO_2=grey, low CO_2=green, fjord water=black. Squares=day 9, diamonds=day 11, triangles=day 13, circles=day 23. Error bars denote precision of the analysis.

BGD
6, 6781–6802, 2009

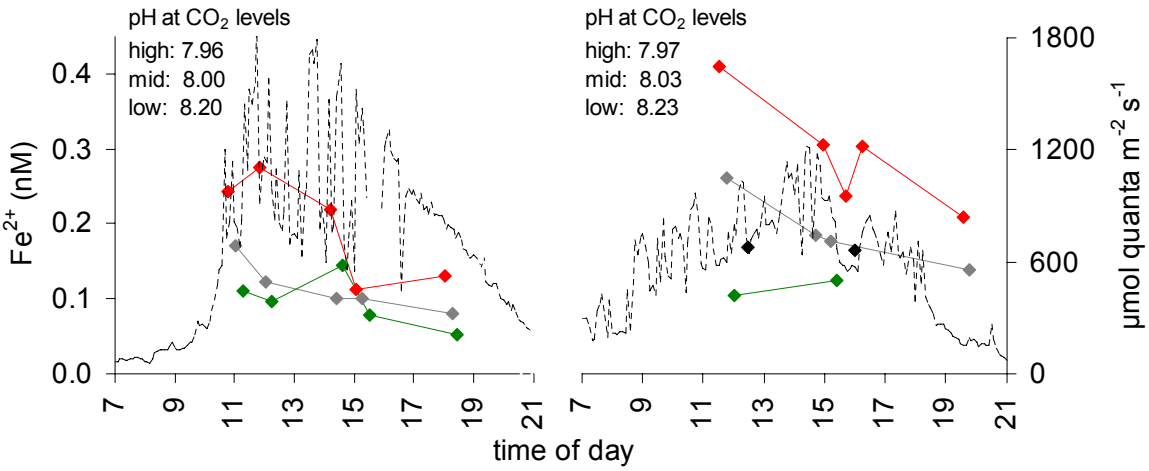

Fig. 5. Fe^{2+} at high (red), mid (grey), low CO_2 (green), and in fjord water (black) and light intensity (dotted line) during days 20 (left) and 22 (right).

BGD
6, 6781–6802, 2009

Ocean acidification affects iron speciation in seawater

E. Breitbarth et al.

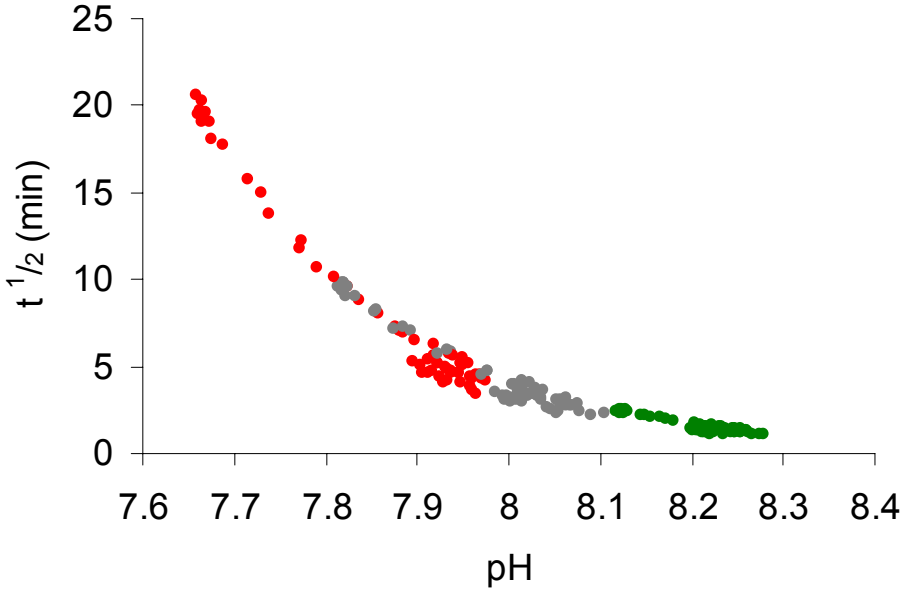

Fig. 6. Predicted Fe(II) half-life times as a function of pH over the course of the mesocosm experiment calculated based on (Millero et al., 1987).

BGD
6, 6781–6802, 2009

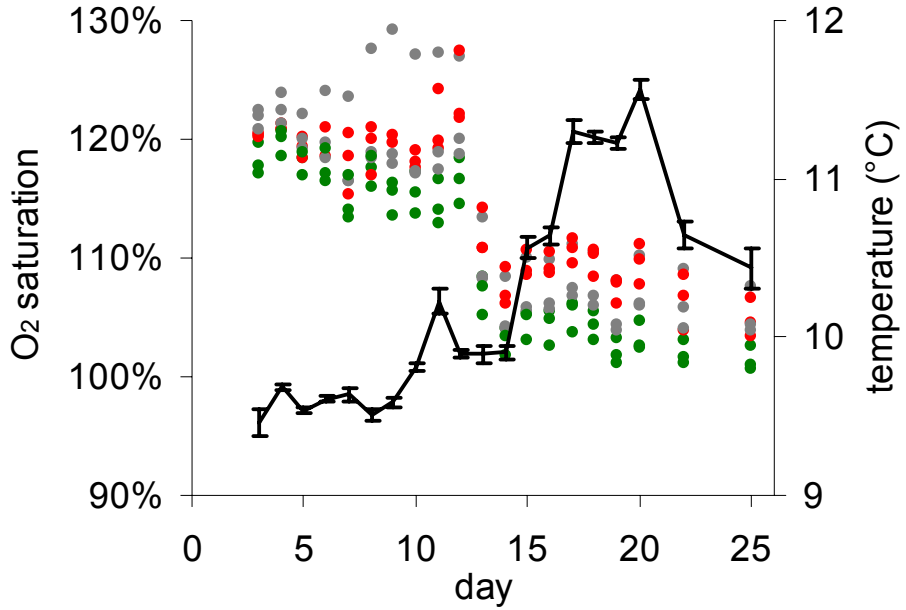

Fig. 7. Oxygen saturation and temperature as a function of time during the mesocosm experiment. For oxygen saturation: high CO_2=red, mid CO_2=grey, low CO_2=green. The relatively high oxygen saturation values in the mid CO_2 treatment (day 5–12) originate from enclosure # 4, which was not used for the discrete Fe(II) samples discussed in this work. The overall mean temperatures of all nine enclosures are shown as a black line (error bars are standard deviations).

BGD
6, 6781–6802, 2009